

A Monte Carlo Study of a Model of Globular Protein Nanoparticles

D. L. Pagan*, M. E. Gracheva**, and J. D. Gunton*

* Department of Physics
Lehigh University, Bethlehem, PA, USA

** Department of Mathematics
University of Minnesota, Minneapolis, MN, USA

ABSTRACT

We explore the metastable fluid-fluid coexistence curve of the modified Lennard-Jones model of globular proteins of ten Wolde and Frenkel [4]. Using grand canonical Monte Carlo simulations along with mixed-field finite-size scaling and histogram reweighting, we estimate the critical temperature to be $T_c^*(\infty) = .4145(5)$ at infinite volume. The subcritical region of the metastable fluid-fluid coexistence curve is obtained using the hyper-parallel tempering method. In close proximity to the critical point, a region previously unattained by simulation, the phase diagram is calculated.

Keywords: nanoparticle, self-assembly, Monte Carlo, proteins

1 INTRODUCTION

Many diseases are known to be caused by the crystallization of certain globular proteins. For example, it has been shown that sickle cell anemia [1] begins with the onset of crystallization of the mutant hemoglobin-S molecule. Other diseases that exhibit this type of morphology include genetic cataracts [2] and Alzheimer's disease. Recent work [3] has focused on understanding the conditions which give rise to the crystallization of such proteins, in order to ultimately prevent the onset of such diseases.

Globular proteins are nanoparticles that self-assemble to form crystals. They are known to have a range of attractive interaction that is small in comparison with the size of the proteins. This is in sharp contrast to much smaller particles such as argon, whose properties have been more extensively studied. Both simulation [4] and theory [5] have predicted that the crystallization of these nanoparticles is optimized in the vicinity of a metastable, fluid-fluid critical point. An accurate determination of the critical point and the phase diagram in the nearby region, then, is needed to precisely identify the conditions of this optimization. We use a model of globular proteins [4] known to capture experimentally determined characteristics, the pairwise energy of which is shown in Eq. (1):

$$V(r) = \begin{cases} \infty, & r < \sigma \\ \frac{4\epsilon}{\alpha^2} \left(\frac{1}{[(r/\sigma)^2 - 1]^6} - \frac{\alpha}{[(r/\sigma)^2 - 1]^3} \right), & r \geq \sigma \end{cases} \quad (1)$$

where σ denotes the hard-core diameter of the particles, r is the interparticle distance, and ϵ is the well depth. The width of the attractive well can be adjusted by varying the parameter α ; for $\alpha = 50$, the resulting phase diagram was found to map to that of globular proteins determined experimentally [3]. We determine the metastable fluid-fluid critical point of the above model using finite-size scaling techniques adapted for simple fluids by Bruce and Wilding [6] and determine the corresponding binodal curve near the critical point using the hyper-parallel tempering method [7].

2 MODEL

Grand canonical Monte Carlo simulates a system at constant volume $V = L^d$, chemical potential μ , and temperature T while the number of particles N is allowed to fluctuate. The joint probability distribution of the number-density $\rho = L^{-d}N\sigma^d$ and energy-density $u = UL^{-d}$ at a particular point in parameter space (β, μ) is analyzed, where U is the total pair-wise energy and $\beta = 1/k_B T$. We then obtain the joint probability distribution of mixed operators

$$P_L(\mathcal{M}, \mathcal{E}) = (1 - sr) P_L(\rho, u), \quad (2)$$

where

$$\mathcal{M} = \frac{1}{1 - sr} [\rho - su] \quad (3)$$

and

$$\mathcal{E} = \frac{1}{1 - sr} [u - r\rho] \quad (4)$$

are the ordering and energy-like operators, respectively, with the parameters s and r system-dependent field-mixing parameters. In simple fluids, or off-lattice models, there is an absence of particle-hole symmetry which gives rise to an asymmetrical density distribution. Analyzing the joint-operator distribution allows one to recover a symmetrical distribution, accounting for mixed-field scaling effects. At criticality, the ordering-operator distribution obeys a scaling relation [6] of the form

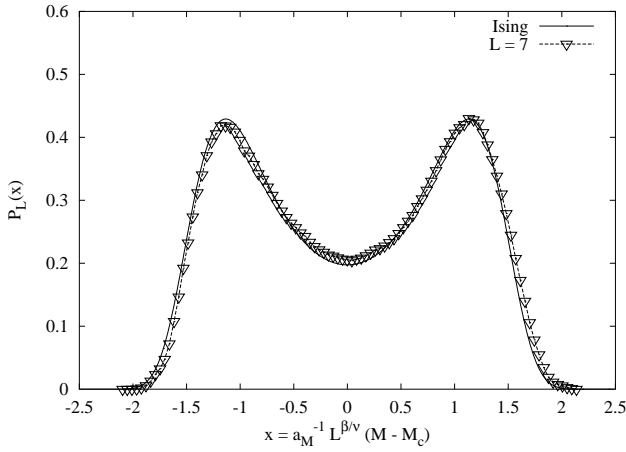


Figure 1: The form of the ordering operator distribution $P_L(\mathcal{M})$ for the $L = 7$ system size. Shown for comparison is the universal Ising fixed-point ordering operator distribution $\tilde{P}_{\mathcal{M}}^*(x)$ (solid). The data has been expressed in terms of the scaled variable $x = a_{\mathcal{M}}^{-1} L^{\beta/\nu} (\mathcal{M} - \mathcal{M}_c)$, where $a_{\mathcal{M}}^{-1}$ was chosen such that the distribution has unit variance.

$$P_L(\mathcal{M}) = \tilde{P}_{\mathcal{M}}^*(a_{\mathcal{M}}^{-1} L^{(d-1/\nu)} [\mathcal{M} - \langle \mathcal{M} \rangle_c]), \quad (5)$$

where $a_{\mathcal{M}}^{-1}$ is a non-universal scaling factor, d is the dimensionality of the system, ν is a critical exponent [8], and the symbol $\langle \rangle_c$ denotes a grand canonical average taken at criticality. It has been shown [9]–[11] that simple fluids belong to the Ising universality class. Matching the fluid fixed point distribution $P_L(\mathcal{M})$ to that of the Ising model at criticality, then, allows for an accurate determination of the critical point parameters.

In the subcritical region, sampling the joint distribution of coexisting phases becomes prohibitively difficult. In this region, a free-energy barrier exists that can no longer be overcome by the now low density fluctuations. We use hyper-parallel tempering Monte Carlo (HPTMC) [7] to tunnel through this barrier. Parallel-processing is used to set up a composite system of simulations (replicas) at different state points (β, μ) , where the unnormalized probability density of the composite state \mathbf{x} is given by

$$p(\mathbf{x}) = \prod_{i=1}^M \exp[-\beta U(x_i) + \beta \mu N(x_i)], \quad (6)$$

with x_i denoting the state of the i^{th} replica of the M replicas. Two types of trial moves are employed according to the above limiting function: 1) regular insertion/deletion trial moves are attempted within each replica and 2) configuration swaps are attempted between pairs of replicas. To enforce detailed-balance, the

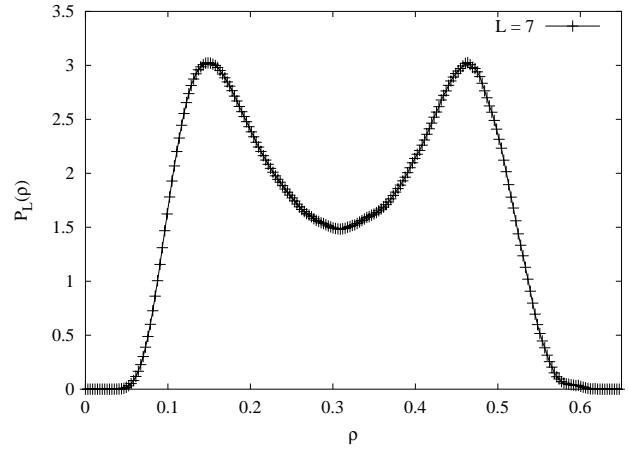


Figure 2: The density distribution for the $L = 7$ system size shown at the critical point $T_c^*(L = 7) = .4130(2)$.

pair of replicas to be swapped are chosen at random and are accepted with the probability

$$p_{acc}(x_i \leftrightarrow x_{i+1}) = \min[1, \exp(\Delta\beta\Delta U - \Delta(\beta\mu)\Delta N)], \quad (7)$$

where $\Delta\beta = \beta_{i+1} - \beta_i$, $\Delta U = U(x_{i+1}) - U(x_i)$, $\Delta(\beta\mu) = \beta_{i+1}\mu_{i+1} - \beta_i\mu_i$, and $\Delta N = N(x_{i+1}) - N(x_i)$.

Both in the critical and subcritical regions, we employ histogram reweighting [12] to facilitate the analysis. Histogram reweighting allows one to extract accurate information about neighboring state points (β', μ') from one single simulation run at a specific set of state points (β, μ) .

The potential in Eq. (1) was truncated at a cut-off distance $r_c = 2.0\sigma$ and left unshifted. Simulations were performed on system sizes of $L = 6\sigma, 7\sigma, 8\sigma$, and 10σ . The systems were equilibrated at two million steps and production runs ranged from 500 million steps to 1 billion steps for the smaller and higher system sizes, respectively. The chemical potential was tuned until a double-peaked structure was obtained in the density distribution in the vicinity of the critical point. We then matched $P_L(\mathcal{M})$ to the Ising distribution as described above. This procedure was repeated for all system sizes studied. In the subcritical region, six replicas were used to obtain coexistence for the $L = 7\sigma$ system. Lower temperatures were biased toward a high density distribution while those at higher temperatures were biased toward a low density distribution. This allowed for swapped configurations to 'melt' more easily. We chose our temperatures and chemical potentials so that many swaps were realized; on average, swaps were accepted 25 percent of the time.

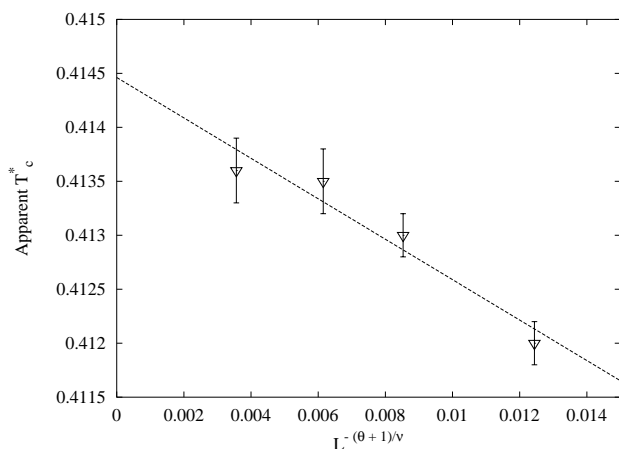


Figure 3: The apparent reduced critical temperature plotted as a function of $L^{-(\theta+1)/\nu}$, with $\theta = 0.54$ and $\nu = 0.629$. The extrapolation to infinite volume yields the estimate $T_c^*(\infty) = .4145(5)$.

3 RESULTS

In Figure 1, we match our order-operator distribution to that of the Ising model. For clarity, only the matching for the $L = 7$ system size is shown. As can be seen, the agreement between the two is good, giving us estimated values of the critical parameters for the $L = 7$ system size of $T_c^*(L) = .4130(2)$ and $\rho_c^*(L) = .312(2)$. In Figure 2, we show the corresponding density distribution for the $L = 7$ system at criticality. By carrying out our simulations at different system sizes, we are able to determine the infinite-volume critical temperature $T_c^*(\infty)$. Deviations from the true critical point are of the form

$$T_c^*(\infty) - T_c^*(L) \propto L^{-(\theta+1)/\nu}. \quad (8)$$

In Figure 3, we plot the apparent critical temperature $T_c^*(L)$ versus $L^{-(\theta+1)/\nu}$. Extrapolation to infinite volume gives us the estimate for the true critical temperature $T_c^*(\infty) = .4145(5)$.

Using HPTMC, density distributions in the subcritical region in close proximity to the critical point were obtained for the $L = 7$ system size. In Figure 4, we plot the temperatures of our six replicas as a function of the average densities of the density distributions to obtain this portion of the phase diagram. Also shown is a power law fit of the form $\rho_{\pm} - \rho_c = A|T - T_c| \pm B|T - T_c|^{\beta}$, where T_c and ρ_c are our extrapolated values as $L \rightarrow \infty$ and $\beta = .3258$ [8] is the Ising exponent, mapping out the rest of the metastable region. From our grand canonical Monte Carlo simulations, we were able to obtain the fluid coexistence curve; also shown is our extrapolated values for the solid coexistence curve. These results match well the previous results of ten Wolde and

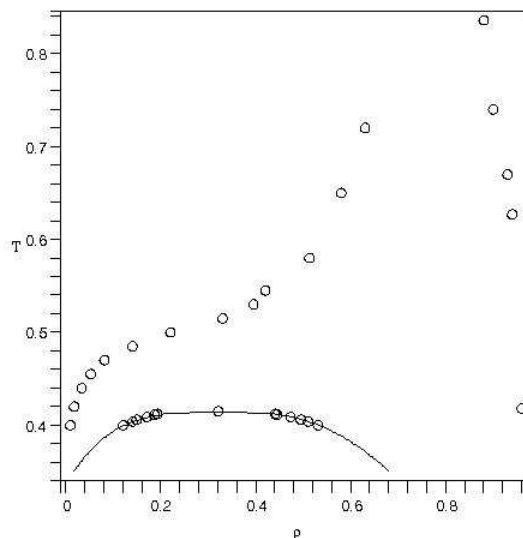


Figure 4: Phase diagram as obtained from both HPTMC and grand canonical Monte Carlo simulations for the $L = 7$ system size shown with the critical point $T_c^*(\infty)$ and the corresponding critical density ρ_c . Also shown (solid line) is a fit to the data, with $\beta = .3258$, the fluid coexistence curve, and extrapolated values for the solid coexistence curve.

Frenek [4]. The metastable data provide a reasonable match to the power-law fit, though we have not accounted for possible finite-size effects.

4 CONCLUSION

Mixed-field finite-size scaling techniques and histogram extrapolation methods were used to estimate the critical-point parameters of the modified Lennard-Jones model [4] of globular proteins. Our estimate for the infinite-volume temperature is $T_c^*(\infty) = .4145(5)$, slightly lower than a previous estimate. In the nearby subcritical region, we explored the phase diagram in close proximity to the critical point, a region previously unattained by simulation. Further details of this work are given in [13].

Many experimental studies have shown that nucleation of protein crystals is indeed enhanced near the critical point. They have also found, however, that globular proteins tend to form gels in part of this region. In a similar system of adhesive spheres, it was recently determined that the critical point lies within the percolation curve [14]. There is no pathway to form gels for the current model, though mode coupling theories describe the gelation region for other similar systems. Obtaining the 'gel-line' as described by mode coupling theory would resolve these differences.

ACKNOWLEDGEMENT

This work was supported by a grant from the National Science Foundation, DMR-0302598.

REFERENCES

- [1] O. Galkin, et al., PNAS **99**, 8479 (2002)
- [2] Ajay Pande, et al., PNAS **98**, 6116 (2001)
- [3] D. Rosenbaum, P.C. Zamora, and C.F. Zukoski, Phys. Rev. Lett., **76**, 150 (1996)
- [4] P. R. ten Wolde and D. Frenkel, Science, **277**, 1975 (1997)
- [5] D. W. Oxtoby and V. Talanquer, J. Chem. Phys., **101**, 223 (1998)
- [6] N. B. Wilding, Phys. Rev. E, **52**, 602 (1995)
- [7] Qiliang Yan and Juan J. de Pablo, J. Chem. Phys., **111**, 9509 (1999)
- [8] A. M. Ferrenberg and D. P. Landau, Phys. Rev. B, **44**, 5081 (1991)
- [9] M. W. Pestak and M. H. W. Chan, Phys. Rev. B, **30**, 274 (1984)
- [10] U. Närgel and D. A. Balzarani, Phys. Rev. B **42**, 6651 (1990); U. Närgel, J. R. de Bruyn, M. Stein, and D. A. Balzarini, *ibid.* **39**, 11 914 (1989)
- [11] J. V. Sengers and J. M. H. Lefelt Sengers, Annu. Rev. Phys. Chem. **37**, 189 (1986)
- [12] A. M. Ferrenberg and R. H. Swendsen, Phys. Rev. Lett., **61**, 2635 (1988)
- [13] D. L. Pagan, M. E. Gracheva, and J. D. Gunton, submitted for publication, Los Alamos preprint 0311551
- [14] Mark A. Miller and Daan Frenkel, Phys. Rev. Lett., **90**, 135702 (2003)